

SANDIA REPORT

SAND2008-5518

Unlimited Release

Printed August 2008

Supersedes SAND2006-3750

dated June 2006

Finite Element Analyses of Continuous Filament Ties for Masonry Applications: Final Report for The Arquin Corporation

Clifford K. Ho, Tiffany A. Bibeau, and Armando Quinones Sr.

Prepared by
Sandia National Laboratories
Albuquerque, New Mexico 87185 and Livermore, California 94550

Sandia is a multiprogram laboratory operated by Sandia Corporation,
a Lockheed Martin Company, for the United States Department of Energy's
National Nuclear Security Administration under Contract DE-AC04-94AL85000.

Approved for public release; further dissemination unlimited.



Sandia National Laboratories

Issued by Sandia National Laboratories, operated for the United States Department of Energy by Sandia Corporation.

NOTICE: This report was prepared as an account of work sponsored by an agency of the United States Government. Neither the United States Government, nor any agency thereof, nor any of their employees, nor any of their contractors, subcontractors, or their employees, make any warranty, express or implied, or assume any legal liability or responsibility for the accuracy, completeness, or usefulness of any information, apparatus, product, or process disclosed, or represent that its use would not infringe privately owned rights. Reference herein to any specific commercial product, process, or service by trade name, trademark, manufacturer, or otherwise, does not necessarily constitute or imply its endorsement, recommendation, or favoring by the United States Government, any agency thereof, or any of their contractors or subcontractors. The views and opinions expressed herein do not necessarily state or reflect those of the United States Government, any agency thereof, or any of their contractors.

Printed in the United States of America. This report has been reproduced directly from the best available copy.

Available to DOE and DOE contractors from
U.S. Department of Energy
Office of Scientific and Technical Information
P.O. Box 62
Oak Ridge, TN 37831

Telephone: (865) 576-8401
Facsimile: (865) 576-5728
E-Mail: reports@adonis.osti.gov
Online ordering: <http://www.osti.gov/bridge>

Available to the public from
U.S. Department of Commerce
National Technical Information Service
5285 Port Royal Rd.
Springfield, VA 22161

Telephone: (800) 553-6847
Facsimile: (703) 605-6900
E-Mail: orders@ntis.fedworld.gov
Online order: <http://www.ntis.gov/help/ordermethods.asp?loc=7-4-0#online>



SAND2008-5518
Unlimited Release
Printed August 2008

Supersedes SAND2006-3750
dated June 2006

Finite Element Analyses of Continuous Filament Ties for Masonry Applications: Final Report for The Arquin Corporation

Clifford K. Ho and Tiffany A. Bibeau
Sandia National Laboratories
P.O. Box 5800
Albuquerque, New Mexico 87185
ckho@sandia.gov
(505) 844-2384

Armando Quinones, Sr.
Arquin Corporation
P.O. Box 876
La Luz, NM 88337
aava2003@yahoo.com
(505) 434-9590

Abstract

Finite-element analyses were performed to simulate the response of a hypothetical vertical masonry wall subject to different lateral loads with and without continuous horizontal filament ties laid between rows of concrete blocks. A static loading analysis and cost comparison were also performed to evaluate optimal materials and designs for the spacers affixed to the filaments. Results showed that polypropylene, ABS, and polyethylene (high density) were suitable materials for the spacers based on performance and cost, and the short T-spacer design was optimal based on its performance and functionality. Simulations of vertical walls subject to static loads representing 100 mph winds (0.2 psi) and a seismic event (0.66 psi) showed that the simulated walls performed similarly and adequately when subject to these loads with and without the ties. Additional simulations and tests are required to assess the performance of actual walls with and without the ties under greater loads and more realistic conditions (e.g., cracks, non-linear response).

Acknowledgments

This report supersedes SAND2006-3750 (June 2006). A bug was discovered in CosmosWorksTM 2004 that yielded incorrect values for the factor of safety (FOS). Therefore, the results and simulations presented and discussed in Section 3 have been revised, and the conclusions have been appropriately changed. Special thanks to Carlos Lopez for identifying these issues and providing corrected values in Table 4. We also thank Carlos Lopez and Jason Petti for providing reviews of this revised report.

The authors would like to thank Jennifer Lee Sinsabaugh of the Small Business Assistance Program for supporting the collaboration between Sandia National Laboratories and the Arquin Corporation and for providing administrative assistance during this project. The work described in this report was funded through the New Mexico Small Business Assistance initiative at Sandia National Laboratories. Neither Sandia nor the U.S. Government acquired any rights in any Arquin Corporation intellectual property as a result of this work.

Sandia is a multiprogram laboratory operated by Sandia Corporation, a Lockheed Martin Company for the United States Department of Energy's National Nuclear Security Administration under contract DE-AC04-94AL85000.

Contents

1. Introduction.....	9
2. Evaluation of Plastic Materials and Designs	10
2.1 Analysis of Static Loading Caused by 12-Foot Wall	10
2.2 Cost Analysis of Different Plastic Materials	15
2.3 Material and Design Recommendations.....	16
3. Lateral Loading of Walls With and Without Continuous Filament Ties	16
3.1 Model Approach.....	17
3.1.1 Boundary Conditions	19
3.2 Results and Discussion	19
4. Summary.....	22
5. References.....	22

List of Figures

Figure 1. Left: Prototype designs made of wood for the Arquin spacer. Right: Filaments (ties) comprised of the spacers and 9-gage steel wires are laid on top of a CMU.....	9
Figure 2. Left: Filaments of ties provide spacing and alignment for rows of CMUs. Right: Assembly of CMUs and filaments.....	10
Figure 3. SolidWorks® models of the short T-spacer (top left), long T-spacer (top right), and bowtie spacer (bottom). All dimensions are in inches.	11
Figure 4. Loading conditions for the short T-spacer (top left), long T-spacer (top right), and bowtie spacer (bottom). Green arrows denote constraints; purple arrows denote loads.	12
Figure 5. Representative images from the short T-spacer simulations. Top left: ABS displacement plot. Top right: PVC displacement plot. Bottom left: ABS factor of safety plot. Bottom right: PVC factor of safety plot.....	13
Figure 6. Representative images from the long T-spacer simulations. Top left: polyethylene displacement plot. Top right: PVC displacement plot. Bottom left: polyethylene factor of safety plot. Bottom right: PVC factor of safety plot.	14
Figure 7. Representative images from the bowtie-spacer simulations. Top left: polypropylene displacement plot. Top right: PVC displacement plot. Bottom left: polypropylene factor of safety plot. Bottom right: PVC factor of safety plot.	15
Figure 8. Force generated on a vertical wall as a result of ground acceleration from an earthquake.....	17
Figure 9. Top left: Single steel-wire filament with short T-spacers. Top right: Assembled row with CMU blocks and two filaments (underside view). Bottom left: Mortar cavity for CMU wall with spacers. Bottom right: Assembled wall with filaments and mortar, ready for analysis.....	18
Figure 10. Boundary conditions applied to the simulated CMU wall. Left: 100 mph wind. Right: Seismic event. Green arrows denote restraints. Red arrows denote lateral pressure (loads).	19
Figure 11. Simulated stress distribution and deformation (exaggerated) on a wall without ties for 100 mph wind (0.2 psi). The simulated stress distribution with ties is similar.	21
Figure 12. Simulated resultant displacement (left) and stress distribution (right) of a wall without ties for seismic event (0.66 psi). Simulation with ties yielded similar results.	21

List of Tables

Table 1. Summary of material properties used in the finite-element analyses.	10
Table 2. Static loading results for the different plastic materials and spacer designs.	12
Table 3. Cost comparison of plastics and spacer designs.	16
Table 4. Simulation comparisons between the CMU wall with and without continuous filament ties.	20

1. Introduction

The Arquin Corporation, a New Mexico company, is developing continuous filament ties that are intended to increase the fabricating efficiency and strength of masonry vertical walls comprised of concrete masonry units (CMU) and other materials such as bricks. The ties are composed of spacers affixed to 9-gage steel wire that are laid on top of each row of the wall (Figure 1). The spacers provide accurate spacing and alignment for each CMU or brick that is laid on top, and the assembled ties are also intended to provide additional structural integrity when laid in between each row of the wall (Figure 2).

Arquin contacted Sandia National Laboratories' Small Business Assistance Program to obtain technical assistance in the following areas:

1. *Identification of suitable plastic materials and designs for spacers for optimal performance and lowest cost.* The material should not yield upon static loading under the weight of the wall, and the material should be amenable to injection molding processes.
2. *Evaluation of enhanced structural integrity of walls with ties.* Simulations should be performed to determine if the ties provide additional strength and deformation resistance to lateral loads caused by high winds, nearby explosions, or seismic events.

The remainder of this report presents simulations, analyses, and discussions regarding each of these areas. Simulations of lateral loads on walls with and without the ties assumed static conditions, perfect bonding, and linear material response. Equivalent static loads were used to simulate the high wind and seismic events, but the explosive scenario was deemed to complex for the analyses presented here. Dynamic non-linear simulations would be needed for more rigorous analyses of the performance of walls under dynamic loading conditions such as explosions and to accurately represent the effects with cracking.

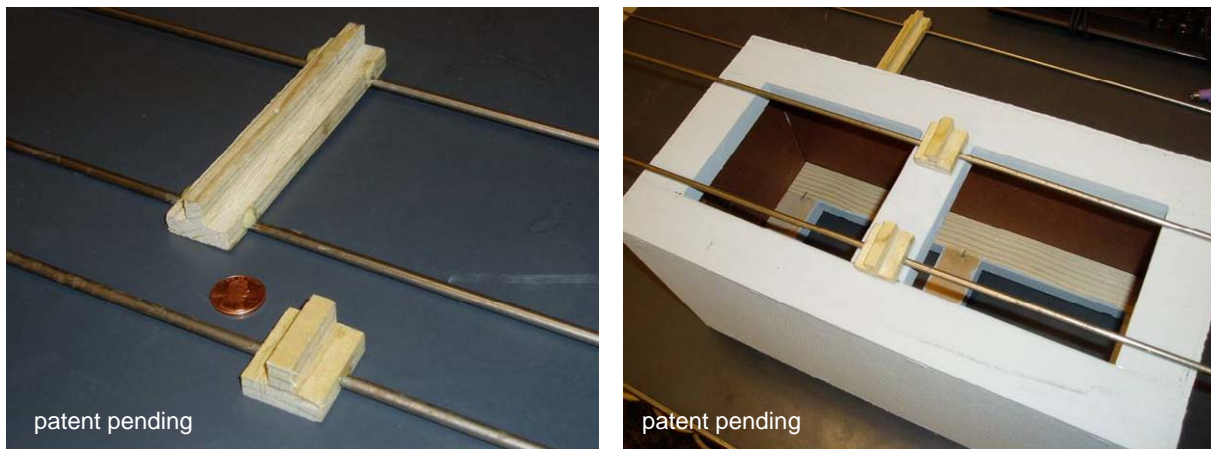


Figure 1. Left: Prototype designs made of wood for the Arquin spacer. Right: Filaments (ties) comprised of the spacers and 9-gage steel wires are laid on top of a CMU.

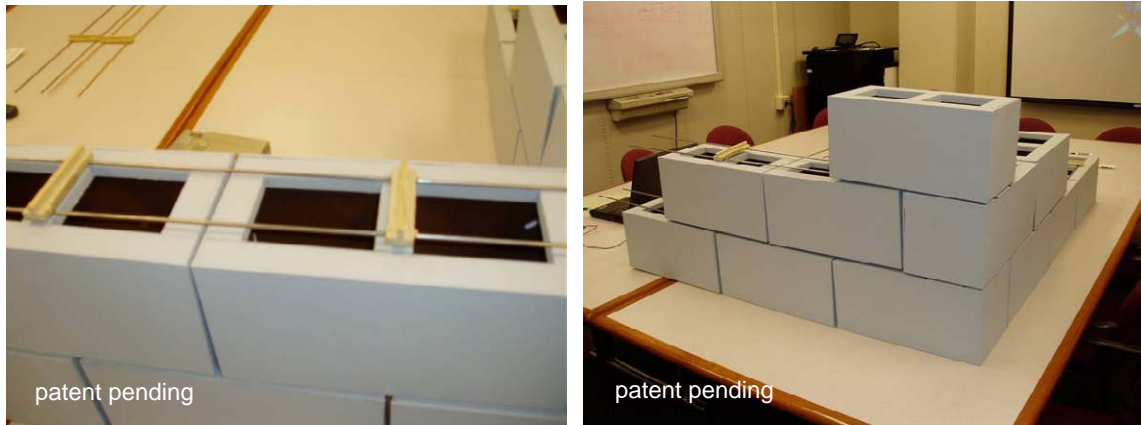


Figure 2. Left: Filaments of ties provide spacing and alignment for rows of CMUs. Right: Assembly of CMUs and filaments.

2. Evaluation of Plastic Materials and Designs

2.1 Analysis of Static Loading Caused by 12-Foot Wall

An analysis was performed to simulate static loading on the spacers caused by a 12-foot high wall. Three different spacer designs were evaluated: (1) short T-spacer, (2) long T-spacer, and (3) bowtie spacer. SolidWorks[®] was used to create three-dimensional models of the different designs (Figure 3). In addition, six different plastic materials were evaluated for each design: polypropylene (PP), acrylonitrile butadiene styrene (ABS), acrylic, polyvinyl chloride (PVC-plasticized), polyethylene (PE-high density), and polytetrafluoroethylene (PTFE or teflon). The material properties used in the analyses are summarized in Table 1.

Table 1. Summary of material properties used in the finite-element analyses.

	Density (kg/m ³):	Modulus of Elasticity (GPa):	Poisson's Ratio:	Yield Strength (MPa):
Concrete ^a	2480	30.0	0.20	37.3*
Mortar ^b	2240	11.17	0.15	12.4*
Polypropylene ^c	905	0.896	0.410	23.8
ABS ^c	1020	2.0	0.394	30.0
Acrylic ^c	1200	2.4	0.350	207
PVC-Plasticized ^c	1290	0.006	0.47	13.0
PE-High Density ^c	952	1.07	0.410	22.1
PTFE ^c	2170	0.40	0.46	20.7
Steel Alloy ^c	7700	211	.28	620

*The strength of concrete and mortar is measured in compression.

^a Callister (2003)

^b Material properties identified by: Portland Cement Assoc. www.cement.org phone: 847.966.6200

^c Material properties identified in SolidWorks[®] 2004 Materials Database (www.solidworks.com).

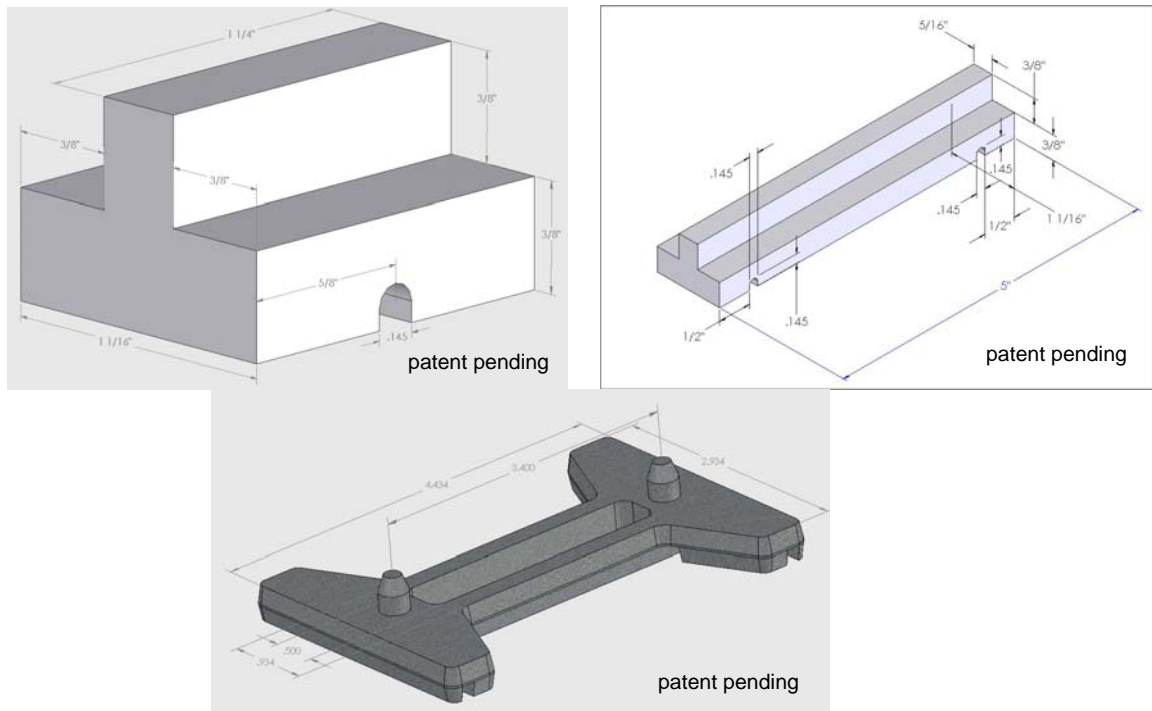


Figure 3. SolidWorks® models of the short T-spacer (top left), long T-spacer (top right), and bowtie spacer (bottom). All dimensions are in inches.

A total loading of 900 lbs was applied to the top surface of each spacer design to simulate the weight of a 12-foot high wall.¹ The load on each surface of the spacer is calculated by dividing the total load by the number of supporting surfaces. For example, each shoulder of the short T-spacer is loaded with 225 lbs. ($900 \div 4$) since the weight of each CMU is supported by a total of four “shoulder” surfaces. The loading on each shoulder of the long T-spacer is 450 lbs since the weight of each CMU is supported by only two shoulder surfaces with the long T-spacer configuration. Finally, the surface of the bowtie spacer is continuous (no shoulders) and supports the entire 900 lbs. The different loadings and the finite-element mesh are shown in Figure 4 for each design. The bottom of each spacer was completely constrained.

CosmosWorks™ 2004 was used to perform a finite-element stress analysis using the boundary conditions identified in Figure 4. Table 2 summarizes the maximum stress, maximum displacement, and minimum factor of safety (FOS) simulated for each of the different materials and spacer designs.

¹ Each CMU weighs approximately 50 pounds, and there are 18 rows in a 12-foot-high wall. Since a spacer is placed on the centerline of each CMU, the weight sustained by the bottom spacer(s) is equal to $18 \times 50 = 900$ pounds.

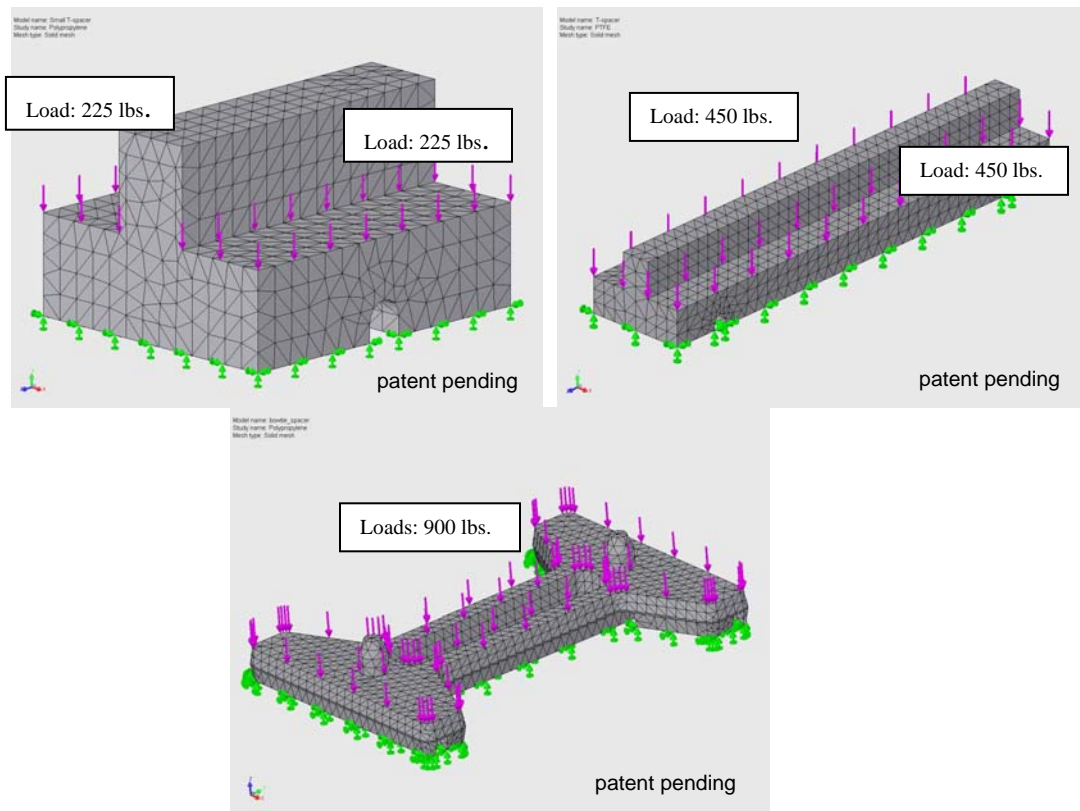


Figure 4. Loading conditions for the short T-spacer (top left), long T-spacer (top right), and bowtie spacer (bottom). Green arrows denote constraints; purple arrows denote loads.

Table 2. Static loading results for the different plastic materials and spacer designs.

Design	Result	Material					
		PP	ABS	Acrylic	PVC	PE	PTFE
Short T-spacer	Max. Stress (MPa)	7.128	7.086	7.103	7.345	7.127	7.789
	Max. Displacement (mm)	0.0467	0.0209	0.0175	7.129	0.0391	0.1063
	FOS	3.3	4.2	29	1.8	3.1	2.8
Long T-spacer	Max. Stress (MPa)	3.755	3.744	3.722	3.813	3.755	3.8
	Max. Displacement (mm)	0.0238	0.0105	0.0024	3.725	0.0199	0.0482
	FOS	6.3	8	56	3.4	5.9	5.4
Bowtie Spacer	Max. Stress (MPa)	3.834	3.856	4.188	3.787	3.835	3.715
	Max. Displacement (mm)	0.0207	0.0940	0.0813	2.916	0.0173	0.0439
	FOS	6.2	6.2	49	3.4	5.8	5.6

FOS = factor of safety (yield strength of material divided by maximum applied stress)

The results show that all of the plastic materials except for PVC produce acceptable results with regard to maximum displacement (deformation) and factor of safety. The maximum displacement simulated for PVC is 7 mm for the short T-spacer design and 3-4 mm for the other designs. The simulated factor of safety is at least three for nearly all three designs except for the short T-spacer design using PVC, which yields a factor of safety of 1.8. Figure 5 through Figure 7 show representative images from the static-load simulations. In each figure, a material with acceptable results is shown on the left, and a material with unacceptable results is shown on the right. The images show plots of the displacement distribution and the factor-of-safety distribution on each design for the representative materials.

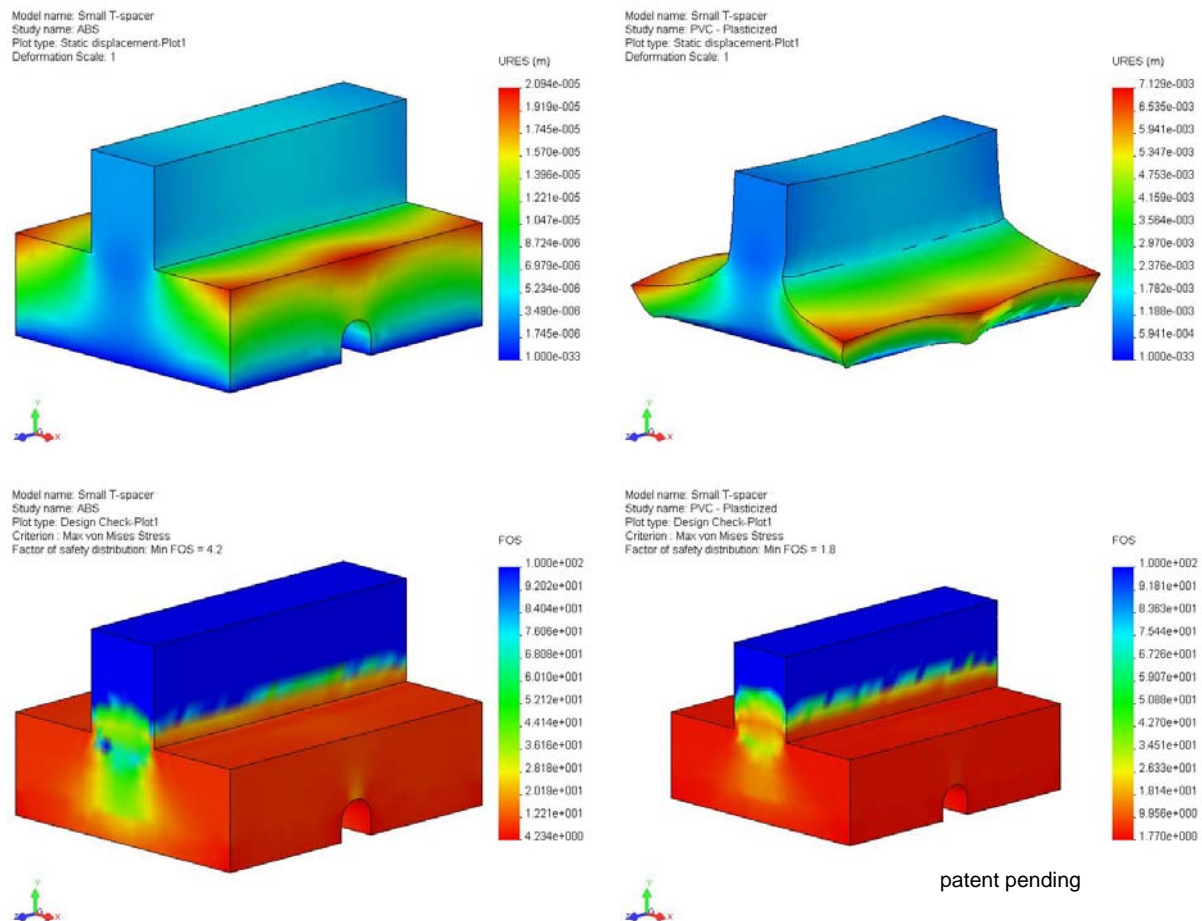


Figure 5. Representative images from the short T-spacer simulations. Top left: ABS displacement plot. Top right: PVC displacement plot. Bottom left: ABS factor of safety plot. Bottom right: PVC factor of safety plot.

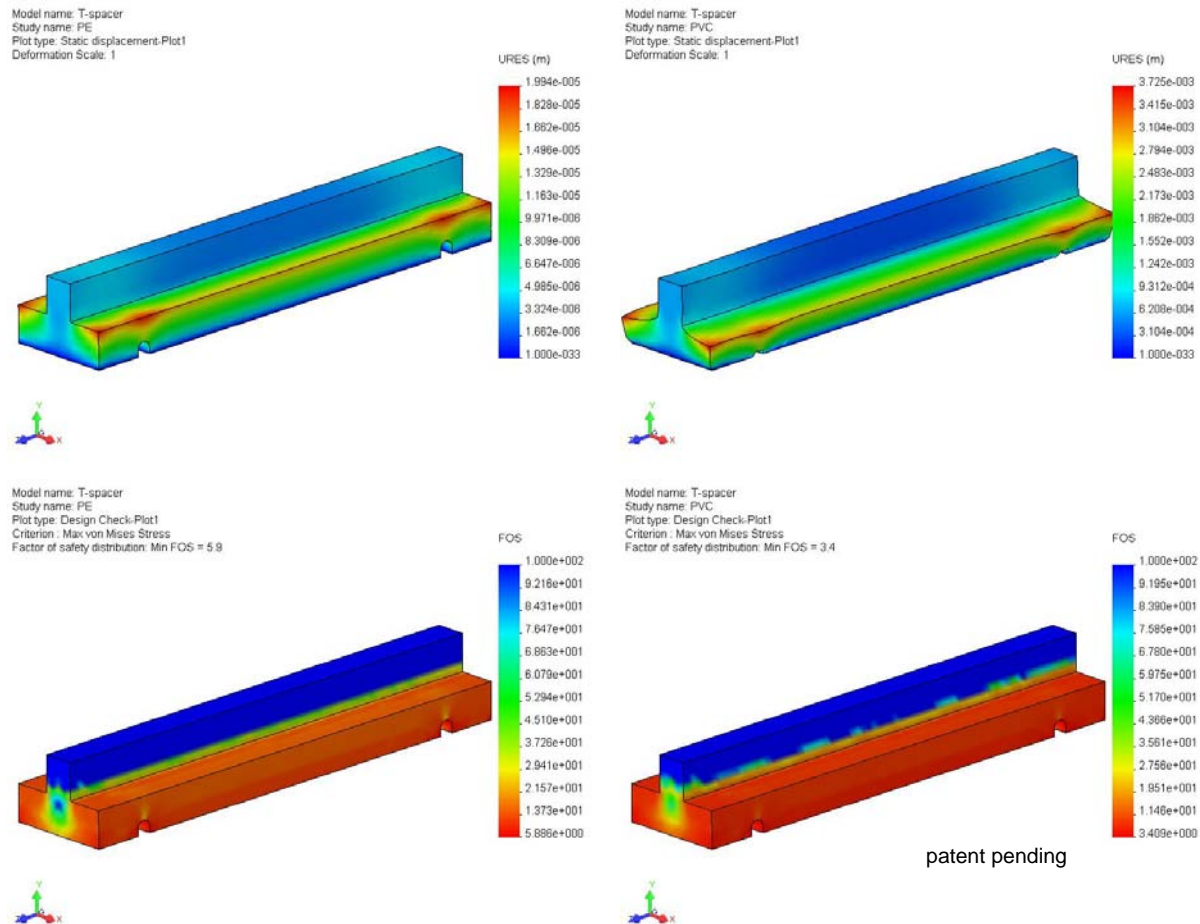


Figure 6. Representative images from the long T-spacer simulations. Top left: polyethylene displacement plot. Top right: PVC displacement plot. Bottom left: polyethylene factor of safety plot. Bottom right: PVC factor of safety plot.

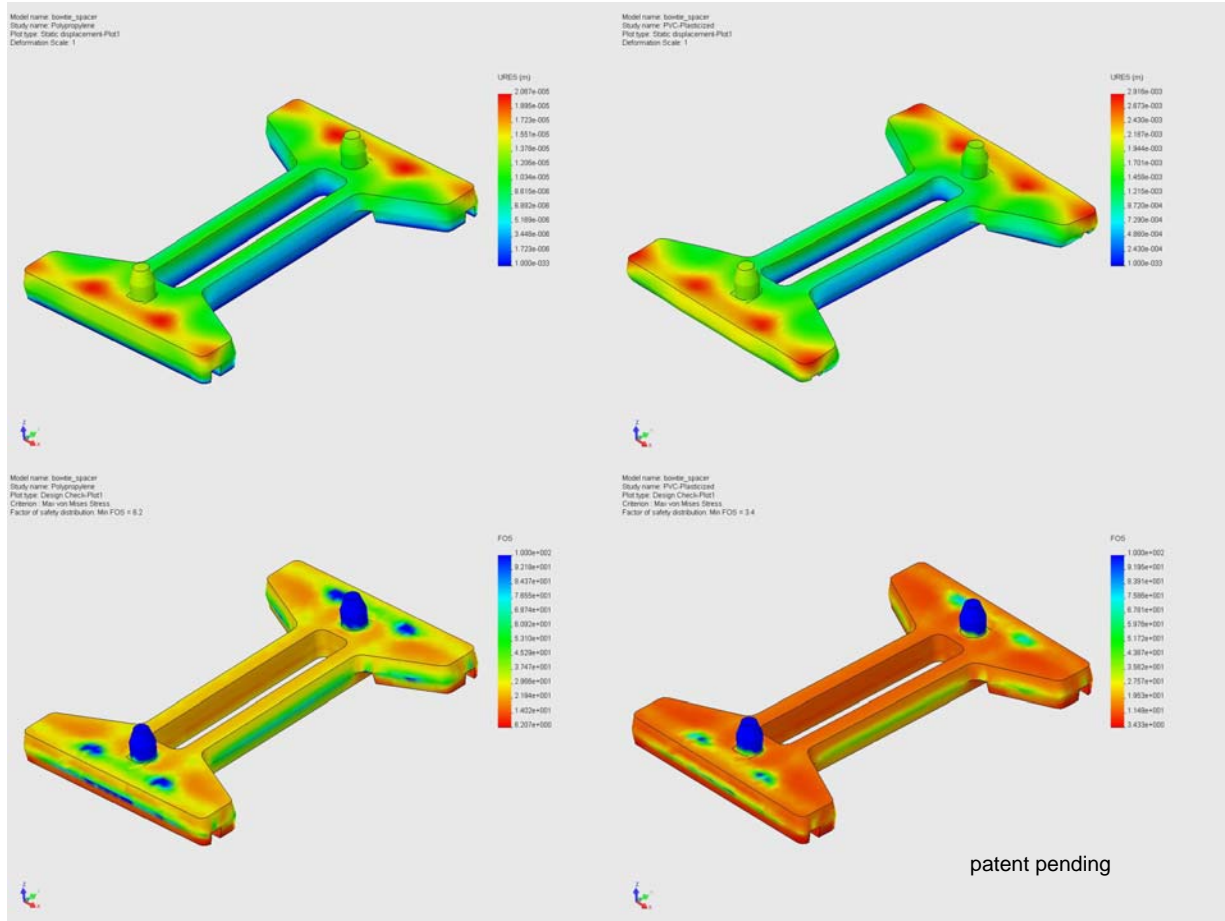


Figure 7. Representative images from the bowtie-spacer simulations. Top left: polypropylene displacement plot. Top right: PVC displacement plot. Bottom left: polypropylene factor of safety plot. Bottom right: PVC factor of safety plot.

2.2 Cost Analysis of Different Plastic Materials

In addition to performance (deformation and factor of safety), cost is another issue that was evaluated among the different materials and designs. Table 3 shows a cost comparison among the materials and designs based on the simulated volume and mass of each part and the reported cost per pound of the different plastics. Polypropylene is the cheapest material, followed by polyethylene, PVC, ABS, acrylic, and then PTFE. Among the different designs, the short T-spacer is the cheapest, followed by the bowtie design and the long T-spacer. The resulting unit cost is for the raw material only, and this price can vary depending on the vendor and the amount of plastic purchased.

Table 3. Cost comparison of plastics and spacer designs.

Design	Feature	Materials Amenable to Injection Molding					
		PP	ABS	Acrylic	PVC	PE	PTFE
Short T-spacer	Volume (cm ³)	10.24	10.24	10.24	10.24	10.24	10.24
	Mass (lbs)	0.02	0.023	0.027	0.029	0.021	0.052
	Cost (per pound)*	\$3.20	\$4.12	\$5.32	\$3.90	\$3.40	\$99.40
	Cost (per unit)	\$0.064	\$0.095	\$0.144	\$0.113	\$0.071	\$5.17
Long T-spacer	Volume (cm ³)	41.59	41.59	41.59	41.59	41.59	41.59
	Mass (lbs)	0.083	0.094	0.110	0.118	0.087	0.213
	Cost (per pound)*	\$3.20	\$4.12	\$5.32	\$3.90	\$3.40	\$99.40
	Cost (per unit)	\$0.266	\$0.387	\$0.585	\$0.460	\$0.296	\$21.17
Bowtie Spacer	Volume (cm ³)	32.20	32.20	32.20	32.20	32.20	32.20
	Mass (lbs)	0.064	0.072	0.085	0.092	0.068	0.165
	Cost (per pound)*	\$3.20	\$4.12	\$5.32	\$3.90	\$3.40	\$99.40
	Cost (per unit)	\$0.205	\$0.297	\$0.452	\$0.359	\$0.231	\$16.40

*Cost per pound of raw material when purchased in small quantities (price will reduce with large quantity orders). KEYTEC, INC. Richardson, TX www.magictouch.com phone: 972.234.8617

2.3 Material and Design Recommendations

Based on the results of the static-loading simulations and the cost comparisons, we recommend the following materials: polypropylene, ABS, and polyethylene (high density). These materials performed well with regard to the simulated performance metrics of displacement and factor of safety, and they were the least expensive. These materials are also amenable to injection molding processes.

With regard to the design, we recommend the short T-spacer design because of its acceptable performance, lowest cost, and the following functionality:

- The single-filament short T-spacer design allows a variable width between two filaments
- More than two filaments can be used depending on pilaster width (e.g., three filaments can be used for wide pilasters)
- Packaging and shipment will be easier with the short T-spacer
- The short T-spacers can be used for single-filament applications (e.g., veneer wall with 2"x4"x8" bricks)

3. Lateral Loading of Walls With and Without Continuous Filament Ties

Simulations were performed to determine if the continuous filament masonry ties provided additional integrity and safety to CMU vertical walls. Lateral loads were applied to the side of a

CMU vertical wall to simulate two different scenarios: (1) 100 mph winds and (2) an earthquake. Masonry walls are typically designed to withstand wind loads up to 100 mph (International Building Code, 2003), which, according to theoretical and empirical drag correlations, corresponds to approximately 0.2 psi of pressure against a flat two-dimensional wall (Roberson and Crowe, 1985).

In addition, ground motion from earthquakes can impose an inertial force on vertical walls that is equivalent to a lateral load (Figure 8). Although many different loading scenarios could be imparted from different types of seismic motions (e.g., P-wave, S-wave, Love Wave, Rayleigh Wave) and spectral energy distributions, the approach taken in this study was to choose a conservative estimate of the peak ground acceleration that could be used to calculate an effective lateral load on the vertical wall. The United States Geological Survey publishes probabilistic seismic hazard assessment maps that give the annual probability of experiencing a particular ground acceleration from earthquakes in various regions. Petersen et al. (1996) report that a peak ground acceleration of 1 “g” (9.81 m/s^2) can be expected to occur in southern California approximately once every thousand years. According to studies by Wald et al. (1999) and Trifunac and Brady (1975), a peak ground acceleration of 9.81 m/s^2 corresponds to a Modified Mercalli Intensity between IX and X, which is comparable to a >7.0 magnitude earthquake on the Richter scale.² This value for the peak ground acceleration was used as an estimate to calculate the applied load that could be experienced by vertical walls during earthquakes.

Simulations of walls subject to these conditions and scenarios were performed with and without the continuous filament ties, and the results were compared.

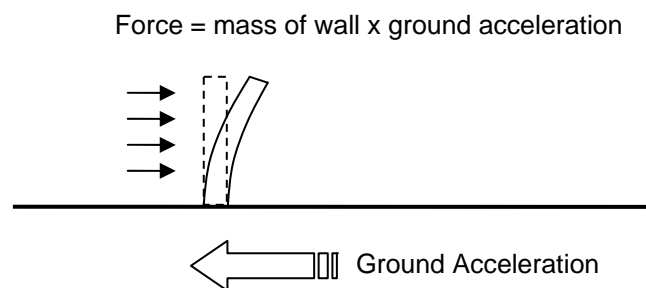


Figure 8. Force generated on a vertical wall as a result of ground acceleration from an earthquake.

3.1 Model Approach

A 4' x 8' wall was constructed in SolidWorks[®] with and without the continuous filament ties. For the model with the ties, the CMU blocks were stacked together and mated to mortar, which filled all the cavities.³ For the model with ties, each filament was simulated, and then a row of CMU blocks was simulated on top of each pair of filaments. The rows were stacked and mortar

² http://earthquake.usgs.gov/learning/topics/mag_vs_int.php

³ All cavities will not be filled during actual construction with the continuous filament ties, but to maintain consistency in the model comparisons, all cavities were assumed to be filled.

was used to fill the cavities (see Figure 9). The total number of elements used in the finite-element simulations for the wall with and without ties was 363,189 elements and 265,059 elements, respectively. The spacer material and design used for the simulations was the polypropylene short T-spacer (two single filaments per row). It was chosen due to its good performance under a static load and low production cost. Table 1 lists the material properties for the polypropylene, concrete, mortar, and steel filaments that were used in the analysis.

CosmosWorks™ 2004 was used to perform static simulations of the lateral loads on the wall. Although the actual loads during wind and seismic events are transient, the loads in the model were assumed to be constant. In addition, the stress-strain response of the materials was assumed to be linear.

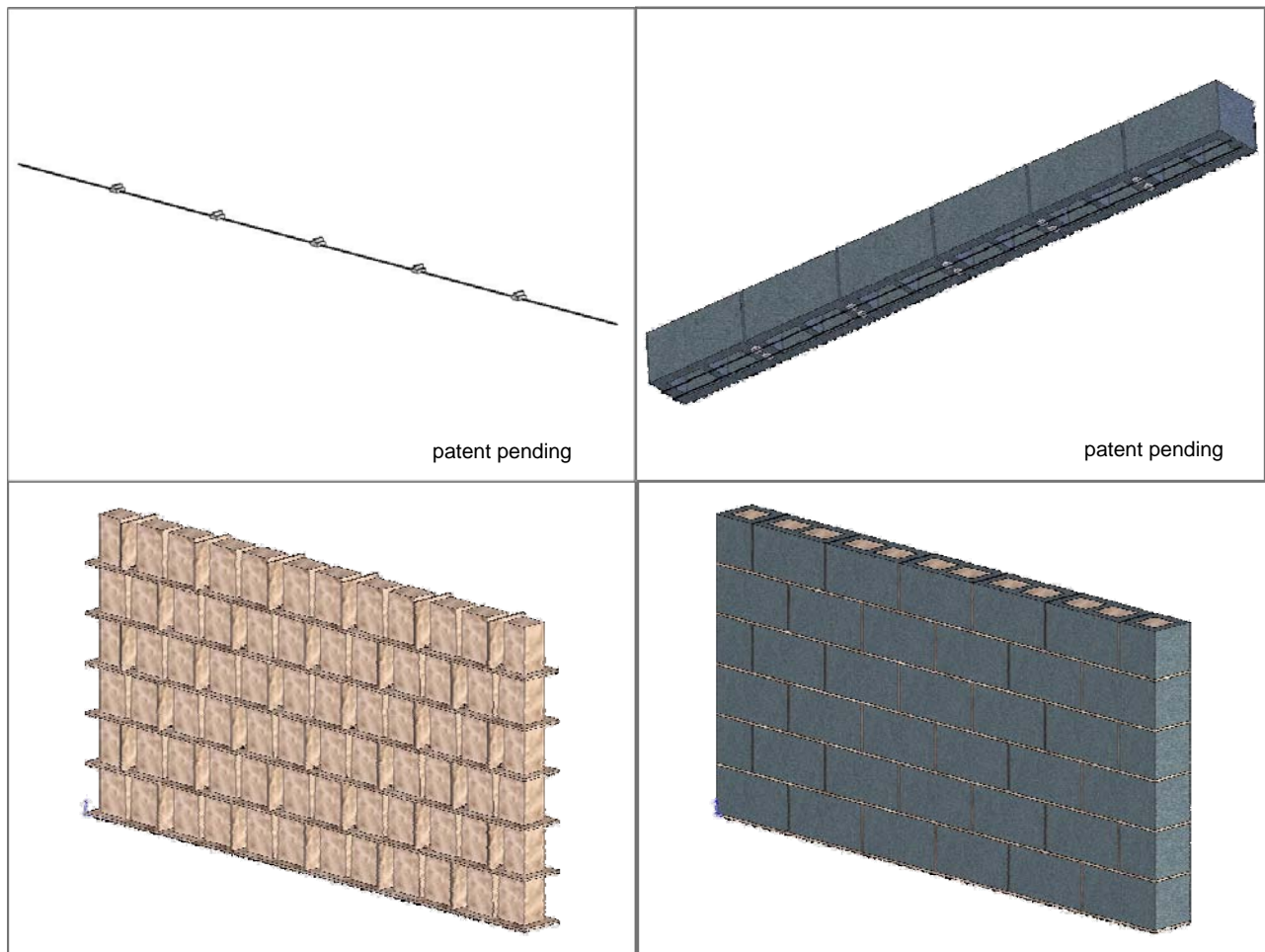


Figure 9. Top left: Single steel-wire filament with short T-spacers. Top right: Assembled row with CMU blocks and two filaments (underside view). Bottom left: Mortar cavity for CMU wall with spacers. Bottom right: Assembled wall with filaments and mortar, ready for analysis.

3.1.1 Boundary Conditions

Different boundary conditions were applied to the simulated wall in the two loading scenarios. For the 100 mph wind scenario, the wall was restrained on the bottom and sides. For the seismic event, the wall was restrained only along the bottom. The difference was due to the assumption that the wind originated from *outside* the wall, and additional perpendicular interior walls provided additional support and restraint along the sides of the wall. In the seismic scenario, it was assumed that the oscillating motion of the ground could cause the vertical wall to move *away* from any interior walls; therefore, only bottom restraints were simulated. A lateral load of 0.2 psi was applied to the face of the vertical wall to represent the high wind. For the seismic scenario, a peak ground acceleration of 9.81 m/s^2 was multiplied by the mass of the wall (1,356 kg) to yield an effective lateral load of 13,300 N ($\sim 3,000 \text{ lb}_f$). Distributed over the area of the wall (3 m^2 or 32 ft^2), the effective pressure applied to the wall was 4580 Pa or 0.66 psi. See Figure 10 for a schematic of the applied boundary conditions for the different scenarios.

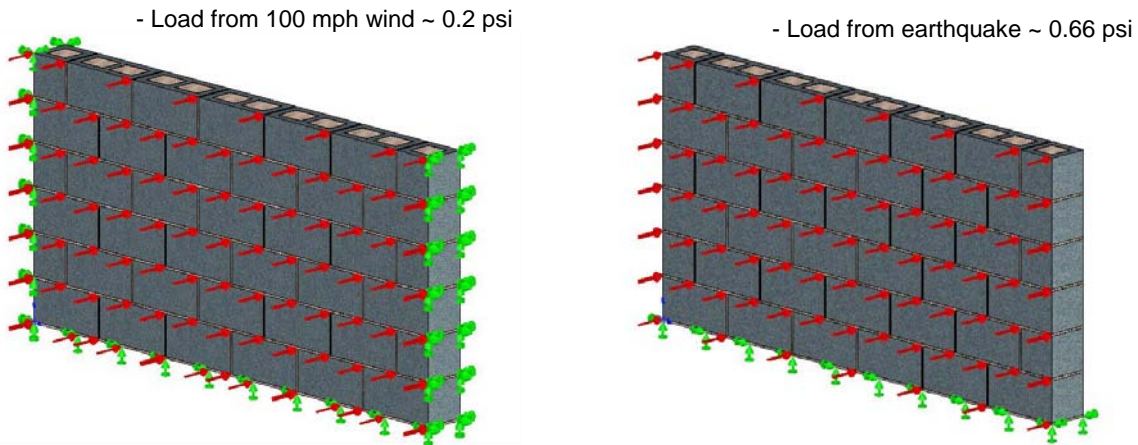


Figure 10. Boundary conditions applied to the simulated CMU wall. Left: 100 mph wind. Right: Seismic event. Green arrows denote restraints. Red arrows denote lateral pressure (loads).

3.2 Results and Discussion

A summary of the simulation results is presented in Table 4. The results show that the simulated wall responds similarly with or without the continuous filament ties when subjected to lateral loads of either 0.2 psi (100 mph wind) or 0.66 psi (seismic event). The simulated maximum displacement is just over 6 microns for the 0.2 psi load and between $\sim 70 - 80$ microns for the 0.66 psi load. The factor of safety (FOS) is above one in all cases. It should be noted that the “yield strengths” for concrete and mortar in Table 1 used in the FOS calculations were measured under compressive loads. For tensile loads, the ultimate strength of these brittle materials will be significantly less (typically $1/10^{\text{th}}$ the compressive strength), so the FOS in tension is estimated to be approximately $1/10^{\text{th}}$ the FOS in compression. In addition, the materials were assumed to be completely intact and perfectly bonded. No cracks were simulated. Therefore, although these walls responded similarly in the simulations, higher loads will likely crack or fail the concrete or

mortar under tension, and the steel filament ties will play a more predominant role in absorbing the tensile loads.

Table 4. Simulation comparisons between the CMU wall with and without continuous filament ties.

	CMU Wall without Continuous Filament Ties	CMU Wall with Continuous Filament Ties (polypropylene spacers)
100 mph wind (pressure = 0.2 psi)		
Max von Mises Stress:	8.7 x 10 ⁴ N/m ² (mortar) 1.2 x 10 ⁵ N/m ² (CMU)	8.7 x 10 ⁴ N/m ² (mortar) 1.3 x 10 ⁵ N/m ² (CMU) 1.9 x 10 ⁵ N/m ² (filament)
Max Displacement:	6.5 x 10 ⁻⁶ m	6.5 x 10 ⁻⁶ m
FOS*:	143 (mortar, compression) ~14 (mortar, tension) 325 (CMU, compression) ~33 (CMU, tension)	143 (mortar, compression) ~14 (mortar, tension) 295 (CMU, compression) ~30 (CMU, tension) 3,340 (filament, tension)
Seismic Event (Peak Ground Acceleration = 1 “g” = 9.81 m/s², 0.66 psi)		
Max von Mises Stress:	6.9 x 10 ⁵ N/m ² (mortar) 5.6 x 10 ⁵ N/m ² (CMU)	7.0 x 10 ⁵ N/m ² (mortar) 5.4 x 10 ⁵ N/m ² (CMU) 4.9 x 10 ⁵ N/m ² (filament)
Max Displacement:	8.16 x 10 ⁻⁵ m	6.85 x 10 ⁻⁵
FOS*:	18 (mortar, compression) ~1.8 (mortar, tension) 66 (CMU, compression) ~6.6 (CMU, tension)	18 (mortar, compression) ~1.8 (mortar, tension) 69 (CMU, compression) ~6.9 (CMU, tension) 1,270 (filament)

FOS = factor of safety (yield strength of material divided by maximum applied stress in that material)

CMU = concrete masonry unit

*The factor of safety for mortar and concrete in tension is estimated assuming that the ultimate tensile strength is 1/10th the compressive strength reported in Table 1.

Figure 11 shows the simulated von Mises stress distribution and deformation (exaggerated) for the wall with a lateral load of 0.2 psi (100 mph wind). The von Mises stress that is shown in Figure 11 does not distinguish between compression and tension; it is an equivalent stress calculated from the simulated stress components and is used to assess design safety. Because the wall is assumed to be fixed along the sides and bottom, the simulated stress is greatest in those regions. The stress along these edges (shown in red) is in compression on the side of the wall opposite the load and in tension along the side of the wall that is loaded. The stress near the center and top of the wall is less than along the edges and is in tension on the side opposite the load and in compression on the side that is loaded.

Figure 12 shows the simulated displacement and von Mises stress distribution for the wall subject to a 0.66 psi load (seismic event) with only the bottom boundary fixed. In this scenario, the presence of the horizontal ties is not expected to significantly impact the imparted loads and bending moment about the horizontal (x) axis.

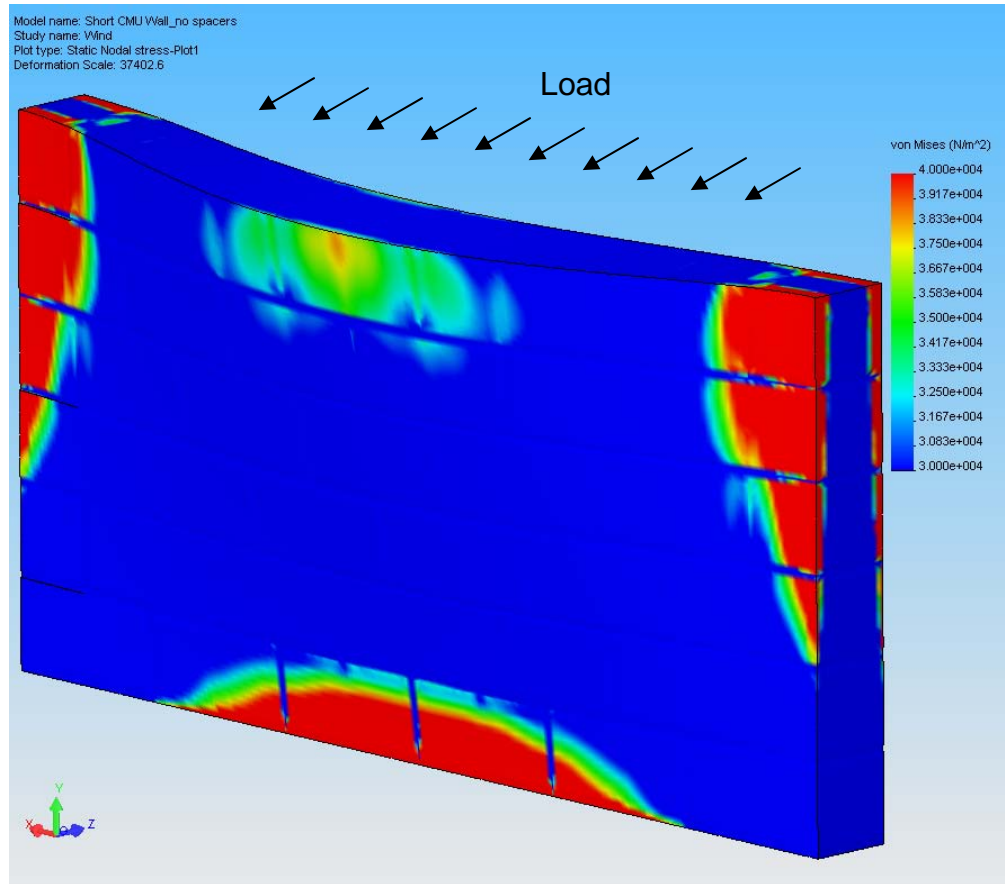


Figure 11. Simulated stress distribution and deformation (exaggerated) on a wall without ties for 100 mph wind (0.2 psi). The simulated stress distribution with ties is similar.

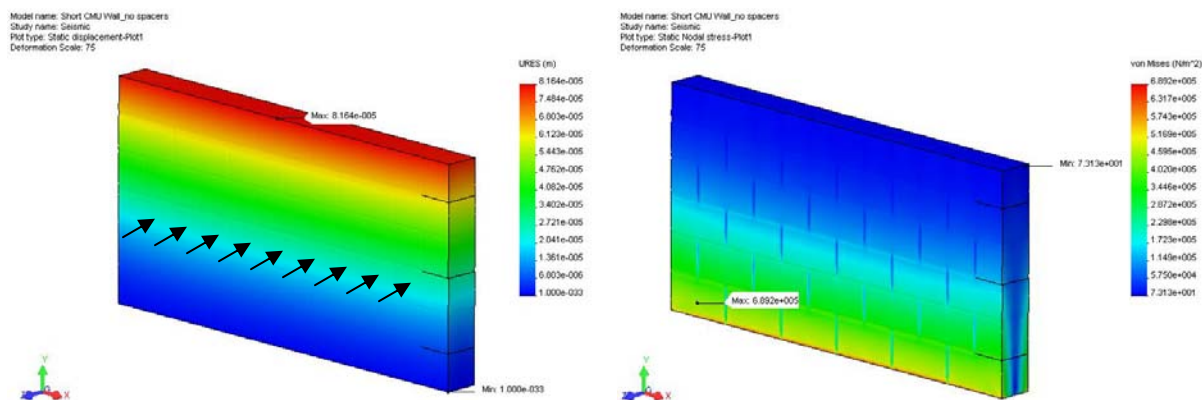


Figure 12. Simulated resultant displacement (left) and stress distribution (right) of a wall without ties for seismic event (0.66 psi). Simulation with ties yielded similar results.

Figure 12 shows that the simulated stress is greatest along the bottom where the wall is fixed. The stress along the bottom of the wall is in tension on the side of the wall that is loaded and in compression on the side of the wall opposite the load. The simulated displacements and stress distribution for walls with and without the continuous filament ties are similar for this scenario.

It should be noted that the models of the static loading scenarios considered in this study may not accurately reflect the response of actual masonry walls subject to similar loading conditions. Constitutive relations governing the behavior of composite materials in contact with each other (e.g., concrete, mortar, steel, polypropylene) were not rigorously defined or evaluated. Materials in contact with each other in the model were assumed to be fixed along the interface. In addition, behavior such as cracking and micro-fracturing and their impact on the overall integrity of the simulated wall were not considered. The purpose was to compare the impacts of various loading conditions on simulated CMU vertical walls with and without the continuous filament ties. All other system parameters and boundary conditions were identical in each pair of simulations. Therefore, a preliminary assessment and comparison of the wall performance with and without the ties could be made. Physical experiments and more rigorous assessments are still needed to assess the performance of walls subject to greater loads and more realistic conditions (e.g., cracks, non-linear response) with and without the continuous filament ties.

4. Summary

Finite-element analyses were performed to assess different materials and designs for proposed continuous filament ties and spacers developed by The Arquin Corporation. Based on the results of the static-loading simulations and cost comparisons, the following materials for the spacer designs are recommended: polypropylene, ABS, and polyethylene (high density). These materials performed well with regard to the simulated performance metrics of displacement and factor of safety, and they were the least expensive. These materials are also amenable to injection molding processes. With regard to the design, the small T-spacer design is recommended because of its acceptable performance, lowest cost, and increased functionality.

Simulations were also performed to evaluate the performance of a wall with and without ties (dual filaments with polypropylene short T-spacers) subject to static loads representing 100 mph winds (0.2 psi) and an earthquake (0.66 psi). Results showed that the simulated walls performed similarly and adequately when subject to these loads with and without the ties. Additional simulations and tests are required to assess the performance of walls with and without the ties under greater loads and more realistic conditions (e.g., cracks).

5. References

Callister, Jr., W.D., 2003, *Materials Science and Engineering, An Introduction*, 6th ed., John Wiley & Sons, New York.

International Building Code, 2003, International Code Council, Inc.

Petersen et al., 1996, Probabilistic Seismic Hazard Assessment for the State of California, United States Geological Survey (USGS) Open-File Report 96-706, U.S. Department of the Interior (online report available at: www.consrv.ca.gov/cgs/rghm/psha/ofr9608/).

Roberson, J.A., and C.T. Crowe, 1985, *Engineering Fluid Mechanics*, 3rd ed., Houghton Mifflin Co., Boston.

Trifunac, M.D. and A.G. Brady, 1975, On the correlation of seismic intensity with peaks of recorded strong ground motion, *Bull. Seismol. Soc. Amer.*, 65, 139-162.

Wald, D.J., V. Quitoriano, T.H. Heaton, and H. Kanamori, 1999, Relationships Between Peak Ground Acceleration, Peak Ground Velocity, and Modified Mercalli Intensity in California, *Earthquake Spectra*, 15(3), 557-564.

Distribution

All Electronic Copies:

1	MS-0735	C. Ho, 6115
1	MS-0744	J. Petti, 6764
1	MS-0718	C. Lopez, 6765
1	MS-0201	J. Sinsabaugh, 10222
1	MS-0899	Technical Library, 9536 (electronic copy)

External (electronic copy)

Armando Quinones Sr.
The Arquin Corporation
P.O. Box 876
La Luz, NM 88337
aava2003@yahoo.com